The Journal of Neuroscience, June 1993, 13(6): 2551–2564

Cellular Distribution of Dopamine D_1 and D_2 Receptors in Rat Medial Prefrontal Cortex

Stephen L. Vincent,[1,3] Yusuf Khan,[3] and Francine M. Benes[1,2,3]

[1]Department of Psychiatry and [2]Program in Neuroscience, Harvard Medical School, Boston, Massachusetts 02115 and [3]Mailman Research Center, Laboratory for Structural Neuroscience, McLean Hospital, Belmont, Massachusetts 02178

The relative distribution and cellular localization of the dopamine D_1 and D_2 receptor subtypes were assessed in frozen sections of rat medial prefrontal cortex (mPFC). The D_1 and D_2 receptor binding sites were labeled with the selective high-affinity antagonists SCH 23390 and *N*-(*p*-aminophenethyl)-spiperone (NAPS), respectively, coupled to either Bodipy or Texas red fluorophores. Under the incubation conditions employed, kinetic, competition, and selectivity studies showed that these modified ligands retained pharmacological selectivity. Optimal binding fluorescence was at 100 nM of each ligand, and fluorescence increased linearly from 1 to 15 min of incubation at 2°C. NAPS–Texas red binding fluorescence was inhibited with 10 nM quinpirole (D_2 agonist), but not 10 nM SKF 38393 (D_1 agonist), while SCH 23390–Texas red binding was inhibited with SKF 38393, but not quinpirole. The localization of dopamine receptor binding was assessed in montages constructed from low-magnification photomicrographs through the depth of the cortex, or in corresponding high-magnification photomicrographs. Cells showing D_1- or D_2-like receptor binding fluorescence were present in layers II–VI, with the highest density observed in layers V and VI. The addition of mianserin (100 nM, 5-HT_2 antagonist) to incubated sections slightly reduced the numbers of labeled cells in each cortical layer, but retained the preferential localization to the deeper layers. Two separate observations supported the idea that the fluorescently coupled ligands were localized to neuronal cell bodies. First, receptor labeling with the fluorescently coupled ligands colocalized almost exclusively to cells in the cortical mantle showing neuron-specific enolase immunoreactivity. Second, a comparison of the cell size distribution taken from adjacent Nissl-stained sections with the size of cells showing D_1- or D_2-like receptor binding fluorescence revealed complete overlapping of fluorescence with neuronal cell bodies. In mPFC layer VI, the size of cells showing D_1-like receptor binding fluorescence was 77.8 ± 5.1 μm^2, similar to nonpyramidal neurons, while that for D_2-like receptor binding fluorescence was 108.2 ± 4.5 μm^2, consistent with both large interneurons and small pyramidal cells. Only a small percentage of cells showing D_1- or D_2-like receptor binding overlapped in size with glia, but this occurred almost exclusively within the white matter region below the cortical mantle. These findings are consistent with the hypothesis that the D_1 and D_2 receptor subtypes are found on different populations of neurons, although some overlap probably occurs. The fact that the laminar distribution of these neurons is similar to that of the mesocortical dopamine afferents suggests that receptor binding activity observed with fluorescently coupled D_1 and D_2 ligands is functionally related to these inputs. Fluorescently coupled ligands for dopamine receptor subtypes may be useful tools for determining how this transmitter system interacts with intrinsic elements of rat mPFC.

[Key words: dopamine receptors, receptor binding, fluorescently coupled ligands, mesocortical dopamine system, medial prefrontal cortex, rat]

The dopamine D_1 and D_2 receptor subtype population (Kebabian and Calne, 1979; Stoof and Kebabian, 1984) in the CNS has been extensively characterized by various approaches, including pharmacological techniques (see reviews by Seeman, 1981; Creese et al., 1983; Hess and Creese, 1987) and molecular cloning (Giros et al., 1990; Sokoloff et al., 1990; Zhou et al., 1990; Sunahara et al., 1991; Van Tol et al., 1991). *In vitro* autoradiographic studies using selective agonists and antagonists have demonstrated regional patterns of localization for D_1 and D_2 receptors in rat (Klemm et al., 1979; Palacios et al., 1981; Dawson et al., 1985; Boyson et al., 1986; Dubois et al., 1986; Charuchinda et al., 1987; Richfield et al., 1989), monkey (Kohler and Radesater, 1986; Richfield et al., 1987; Lidow et al., 1989), and postmortem human brain (Liskowsky and Potter, 1985; Camus et al., 1986; Dawson et al., 1987; De Keyser et al., 1988; Camps et al., 1989; Cortes et al., 1989). These studies show D_1 and D_2 receptors to be present in the basal ganglia, nucleus accumbens, olfactory tubercle, cingulate cortex, and the prefrontal area, sites known to receive dopaminergic projections (Berger, 1977; Emson and Koob, 1978; Lindvall and Bjorklund, 1978; Thierry et al., 1978; Lewis et al., 1988).

Although conventional film autoradiographic techniques have been useful in characterizing the regional distribution of dopamine D_1 and D_2 receptors, this approach does not have sufficient resolution to permit the localization of these receptor subtypes to single neurons in sections of intact brain tissue (Herkenham, 1988). A high-resolution coverslip emulsion technique is ideal for obtaining quantitative binding data from single cells (Young and Kuhar, 1979; Benes et al., 1989), but this approach

Received June 23, 1992; revised Dec. 14, 1992; accepted Dec. 21, 1992.

We thank Dr. Ross J. Baldessarini for his helpful comments on the manuscript. This work has been supported by grants from the National Institute of Mental Health, Level II Research Scientist Development Awards MH00423 and MH31154 (F.M.B.).

Correspondence should be addressed to Francine M. Benes, Mailman Research Center, McLean Hospital, 115 Mill Street, Belmont, MA 02178.

cannot be readily combined with most other standard localization techniques, precluding its widespread use in double-labeling paradigms. An alternative approach that has the potential of providing discrete, high-resolution information regarding the anatomical localization of receptors, and one that may be potentially combined with immunolabeling techniques, is the use of fluorophore-labeled, high-affinity ligands that are specific to various receptor subtypes, including D_1 and D_2 high-affinity sites. Recently, the dopamine D_1 and D_2 receptor antagonists SCH 23390 and *N*-(*p*-aminophenethyl)-spiperone (NAPS), respectively, have become available as fluorescently coupled probes (Monsma et al., 1989). The technique of receptor binding on slide-mounted tissue sections using these fluorescently coupled, high-affinity ligands has been employed to visualize the anatomical distribution of neurons bearing D_1 and D_2 receptor binding sites in corpus striatum and nucleus accumbens of rat forebrain (Ariano et al., 1989, 1991). To date, the distribution of binding for the fluorescently coupled ligands in the medial prefrontal cortex (mPFC), a region known to receive a dopaminergic projection from the A10 cell group of the ventral tegmental area (Lindvall and Bjorklund, 1978; Thierry et al., 1978), has not as yet been characterized. Information regarding the anatomical localization of cortical dopamine receptors may add to our understanding of how midbrain ventral tegmental neurons interact with intrinsic elements of mPFC. In addition, the fact that dopamine-blocking drugs are effective in the treatment of psychosis (Bacopoulos et al., 1979; Matsumoto et al., 1983; Berman et al., 1986) has raised the possibility that localizing such binding activity to specific neuronal subtypes may provide clues concerning the role of dopamine in the pathophysiology of schizophrenia, a disorder in which a relative excess of dopamine-dependent neuronal activity has been postulated by some to be a significant contributing neurochemical defect (Kety and Matthysse, 1972; Meltzer and Stahl, 1976; Carlsson, 1978a,b).

To gain a better understanding of the functional relationship between these receptor sites and intrinsic neuronal elements of the cortex, we examined the use of fluorescently coupled, selective antagonist ligands in characterizing the distribution and cellular localization of dopamine D_1 and D_2 receptor binding fluorescence in the rat mPFC using fluorescently coupled SCH 23390 and NAPS, respectively. Tissues were examined with epifluorescence optics for the presence of cells showing D_1- or D_2-like receptor binding fluorescence in the mPFC to characterize the relative distribution and localization of such cells in cortex.

Materials and Methods

Tissue preparation. Male CD rats (300–400 gm body weight; Charles River Breeding Laboratories, Wilmington, MA) were decapitated, their brains were rapidly removed and cut in a coronal plane at the level of the optic chiasm, and the forebrain block was rapidly frozen in Tissue-Tek O.T.C. Compound (Miles, Elkhart, IN) on crushed dry ice and stored at −75°C. Coronal serial sections, taken at a level rostral to the genu of the corpus callosum, were cut at a thickness of 10 μm at −14°C on a cryostat, and then thaw mounted on gelatin-coated slides, and either used immediately or stored at −20°C for 24 hr.

Dopamine D_1 and D_2 receptor binding. Dopamine D_1 and D_2 receptor binding sites were labeled by using the antagonists SCH 23390 and NAPS, respectively, coupled to either of the fluorophores, Bodipy or Texas red. Stock solutions of the fluoroprobes were prepared in dimethyl sulfoxide (DMSO) and stored at −20°C. Initial binding trials based on the methods described by Ariano et al. (1989, 1991) produced a high background fluorescence that prevented visualization of labeled cells. A procedure that provided relatively consistent and reproducible binding patterns is described below.

All receptor assays were carried out in a 100 mM Tris-HCl buffer, pH 7.4, that contained no additional ions or salts. Tissue sections were transferred through two changes of buffer at 2°C for a total of 5 min in order to rehydrate the tissue and remove endogenous dopamine. The sections were then incubated with a fluorescently coupled ligand, washed three times for 30 sec in fresh buffer, and dipped once (5 sec) in distilled water, at 2°C. The slide-mounted sections were rapidly dried with a stream of air and stored in sealed slide boxes at 4°C until examined the following day.

To determine optimal binding conditions for visualization of fluorescence, a series of experiments were performed to assess the characteristics of fluoroprobe binding. The D_1 series used SCH 23390–Bodipy or SCH 23390–Texas red, and the D_2 assay used NAPS–Texas red or NAPS–rhodamine (Molecular Probes, Eugene, OR) to label the respective receptor binding sites. Studies were performed with concentrations of labeled ligand from 10 to 100 nM to assess the optimal concentration of ligand. Kinetic studies were performed using a 100 nM concentration of labeled ligand, and incubation times varied from 1 to 60 min. Competition studies were carried out using 100 nM labeled ligand with varying concentrations of unlabeled receptor agonist in the incubation solution, using (+)SKF 38393 for D_1 receptors, and quinpirole for D_2 receptors (Research Biochemicals Inc., Natick, MA). In studies that used competitors, the tissues were initially incubated for 10 min in buffer that contained only the competitor, followed by incubation with both the labeled ligand and the competitor. All incubations included 100 nM mianserin-HCl (Research Biochemicals Inc.) to block the binding of ligand to serotonin 5-HT_2 receptors (Palacios et al., 1981; Altar et al., 1985a,b).

For analyses of the laminar distribution of cells showing dopamine-like receptor binding, each receptor subtype was independently labeled by incubating the tissue sections for 10 or 15 min in 100 nM concentrations of the appropriate fluorescently coupled D_1 or D_2 ligands at 2°C. In order to ascertain the effect of mianserin on displacing the binding of the D_2 ligand to 5-HT_2 receptors, an experiment was done with NAPS–Texas red in the presence and absence of 100 nM concentration of mianserin-HCl.

Adjacent tissue sections were stained with cresyl violet for Nissl substance in order to verify anatomically the presence of mPFC and to obtain general cell size and density data. The atlas of Paxinos and Watson (1986) was used to identify relevant structures in the rat brain.

Photography. Dopamine receptor binding fluorescence was viewed using fluorescein isothiocyanate (FITC)- and rhodamine-specific dichroic filters with the epifluorescence optics of a Leitz Diaplan light microscope. The excitation and emission spectra for Bodipy (495/505 nm) and Texas red (594/623 nm) are within the wavelength band widths specified by the FITC- and rhodamine-specific excitation and emission filters. The use of aqueous or oil-based coverslipping media was avoided because it would promote disassociation of the ligands and diffusion of the fluoroprobe in the media, thus making this method of preparation impractical for viewing and subsequent storage of specimens. Under these conditions a "dry" coverslip was placed on the tissue sections prior to viewing in the microscope. Low-power photomontages through the depth of the cortex were constructed from photomicrographs made with a 25× Fluotar lens (0.60 NA). High-magnification photomicrographs were made with a 40× Fluotar lens (0.70 NA), coupled to a 1.6× magnification converter. Photomicrograph exposure times were standardized with the camera in the manual exposure mode (Table 1). Images were recorded using Tri-X Pan black-and-white film developed with Rodinal (Agfa) for high image acutance, at normal plus 20% development time to increase contrast. The negatives were printed on Kodak Polycontrast III RC paper using a high-contrast #5 filter in order to maximize the contrast level between fluoroprobe-positive cells and the background. Because of slight variations in the density of the negatives obtained from each receptor assay, printing exposure times were standardized for each experimental condition to optimize the visualization of receptor-positive cell bodies and to demonstrate accurately the effects of the different experimental conditions. In addition, low-magnification photomontages were made of adjacent, cresyl violet–stained sections from corresponding areas of cortex in order to determine the boundaries of the cortical laminae in the fluorescent photomontages.

Receptor distribution analysis. In order to reduce further the background level of fluorescence and to highlight better the position of labeled cell bodies for counting, the low-power photomontages were photocopied and the resulting sheets were pieced together to form a duplicate

montage. To determine the laminar distribution of cells bearing the labeled dopamine receptor subtypes, drawings were made from the column of cortex illustrated in the duplicate photomontages indicating the location of cells with D_1-like or D_2-like receptor binding fluorescence throughout the depth of the mPFC. The numbers of fluorescence-emitting cell profiles per mm^2 were determined for the cortical laminae grouped together as layers II–III and V–VI. The area for each layer of the cortex in the photographic field was made with a WYSE 386pc computer equipped with BIOQUANT software (R and M Biometrics, Nashville, TN). Cortical lamination was determined from the photomontage made from the corresponding cresyl violet–stained section.

Cell size distributions were obtained from representative fields of layer VI and subcortical white matter that contained D_1- and D_2-positive cells and from adjacent cresyl violet–stained sections. The determination of cell size was carried out with the following steps. Microscopic fields were initially viewed with a 40× Fluotar lens coupled to a 1.25× magnification converter with the aid of a Dage-MTI SIT-68 video camera interfaced with a DSP-100 digital signal processor (DAGE-MTI Inc., Michigan City, IN). A series of fields containing layer VI or subcortical white matter were recorded on a still video floppy disk using a Sony MVR-5300 still video recorder that was operated in the hi-band/frame format for high-resolution recording. Subsequently, these recorded images were transferred to the WYSE 386pc computer and cell size measurements were made using BIOQUANT software. Cell size distributions from adjacent cresyl violet–stained sections were made using a Leitz Laborlux S microscope interfaced with the computer.

Neuron-specific enolase. To establish whether the fluoroprobe-positive cells observed in mPFC were neurons, a colocalization study for dopamine receptor binding fluorescence and neuron-specific enolase (NSE) immunoreactivity (NSE-IR) was carried out. In this procedure, tissue sections containing mPFC were incubated separately with D_1 or D_2 fluoroprobes as described above. Regions of layer VI and subcortical white matter were photographed using epifluorescence optics; the corresponding microscope stage x and y vernier coordinates were noted. Immediately following the photography session for dopamine receptors, the immunolabeling procedure for NSE was carried out on the same tissue sections. This procedure was performed in plastic snap-cap slide holders so that the sections would be uniformly exposed to the various reagents. The sections were first incubated in a solution of 0.03% H_2O_2 in 50 mM Tris-saline buffer (TS), pH 7.4, for 10 min at room temperature. The sections were then washed in TS and exposed for 1 hr to a solution containing 1.3% normal goat serum in TS–0.3% Triton X-100 (TST). Following three washes with TST, the tissue sections were incubated overnight at room temperature in TST, pH 7.4, containing a 1:1500 dilution of rabbit anti-human NSE (Incstar, Stillwater, MN). Following incubation with primary antibody, the sections were washed in TST and then treated for 1.5 hr at room temperature with TST containing 0.05% goat anti-rabbit antibody. The sections were washed in TST and then incubated for 2 hr at room temperature in TST containing the avidin–biotinylated enzyme complex (Vectastain ABC Kit, Vector Laboratories, Inc., Burlingame, CA). Following this incubation, the sections were washed several times in TS and then exposed for 5 min to TS containing 0.05% 3,3′-diaminobenzidine and 0.05% H_2O_2. Sections were washed several times in TS, air dried, dehydrated through alcohol and xylene, and coverslipped with Cytoseal-60 mounting media.

The immunoreacted sections were photographed with a light microscope and Nomarski interference contrast illumination using the previously determined magnification and microscope stage x and y vernier coordinates. Thus, the photographed NSE-immunoreacted areas were identical to those previously taken for the two dopamine receptor subtypes. The corresponding pairs of photographic prints generated from the respective dopamine receptor-labeled/NSE-immunoreacted tissue sections were analyzed for the presence of cells identified by both fluoroprobe and NSE immunoreactivity. A comparative analysis for this dual identification was done for cells in layer VI and the subcortical white matter of mPFC.

Results

Methodological considerations

Initially, it was necessary to establish tissue preparation procedures and assay conditions that would produce pharmacologically appropriate and reproducible fluoroprobe binding to dopamine receptors in the cortex. To preserve the morphological integrity of the tissue, initial experiments were carried out with brains that were lightly fixed by perfusion with buffered 0.1% formaldehyde, followed by immersion in buffered 30% sucrose, and then frozen in Tissue-Tek O.T.C. compound. Results from tissues prepared in this manner were difficult to interpret due to the presence of excessively high, nonspecific background fluorescence that obscured the binding of fluoroprobe on cell bodies. In addition, there were large circular-shaped artifacts of fluoroprobe heterogeneously distributed over the entire surface of the tissue sections, thus rendering these tissues unsuitable for analysis. Subsequent studies were carried out with unfixed, fresh-frozen tissue that provided an optimal fluoroprobe localization with low background labeling, a high degree of probe specificity, and satisfactory preservation of morphological detail. It was also found that using a Tris-HCl buffer, free of other ions or salts, in place of phosphate-buffered saline, further lowered the background fluorescence and improved the morphological integrity of the tissue.

Table 1. Manual exposure times determined for fluorophores and objective magnification factors[a]

	Exposure time (sec)	
Fluorophore	25×[b]	64×[b]
Bodipy	45	80
Texas red	20	45
Rhodamine	20	45

[a] See Materials and Methods for specific details regarding photographic processing.
[b] Objective magnification.

Studies were performed using fluorescently coupled SCH 23390 and NAPS to determine the appropriate concentration of ligand needed to detect D_1-like and D_2-like receptor binding fluorescence, respectively. The results of these assays were obtained by careful analysis of representative fields from photomicrographs where the relative fluorescent emission intensity and localization of fluoroprobe were compared for the different concentrations of ligand. Although some binding fluorescence could be detected with ligand concentrations in the 10–50 nM concentration range, 100 nM proved to be the most reliable concentration of fluoroprobe for detection of cell bodies showing D_1-like or D_2-like binding using conventional photomicrography, while still yielding acceptably low background fluorescence.

Kinetic studies were performed by using a 100 nM concentration of fluoroprobe to determine the appropriate amount of time for the preincubation wash, incubation, and postincubation wash. As determined from analysis of representative photographic fields, a brief wash of the tissue sections through two changes of cold buffer prior to incubation with the respective ligands reduced background fluorescence and increased the apparent intensity of fluorophore emission from fluorescence-emitting cortical cells. For SCH 23390–Bodipy, optimal visualization of labeled cell bodies was attained at 15 min of incubation, while for SCH 23390–Texas red and NAPS–Texas red a 10 min incubation was adequate to produce an appropriate localization (Fig. 1). At 60 min of incubation, the intensity of background fluorescence began to obscure visualization of labeled cells that were present at earlier time points; by 90 min of incubation cell bodies could not be distinguished from surrounding neuropil. In addition, for all binding experiments, it was determined that three postincubation washes of 30 sec duration each were adequate to attain a high degree of specific

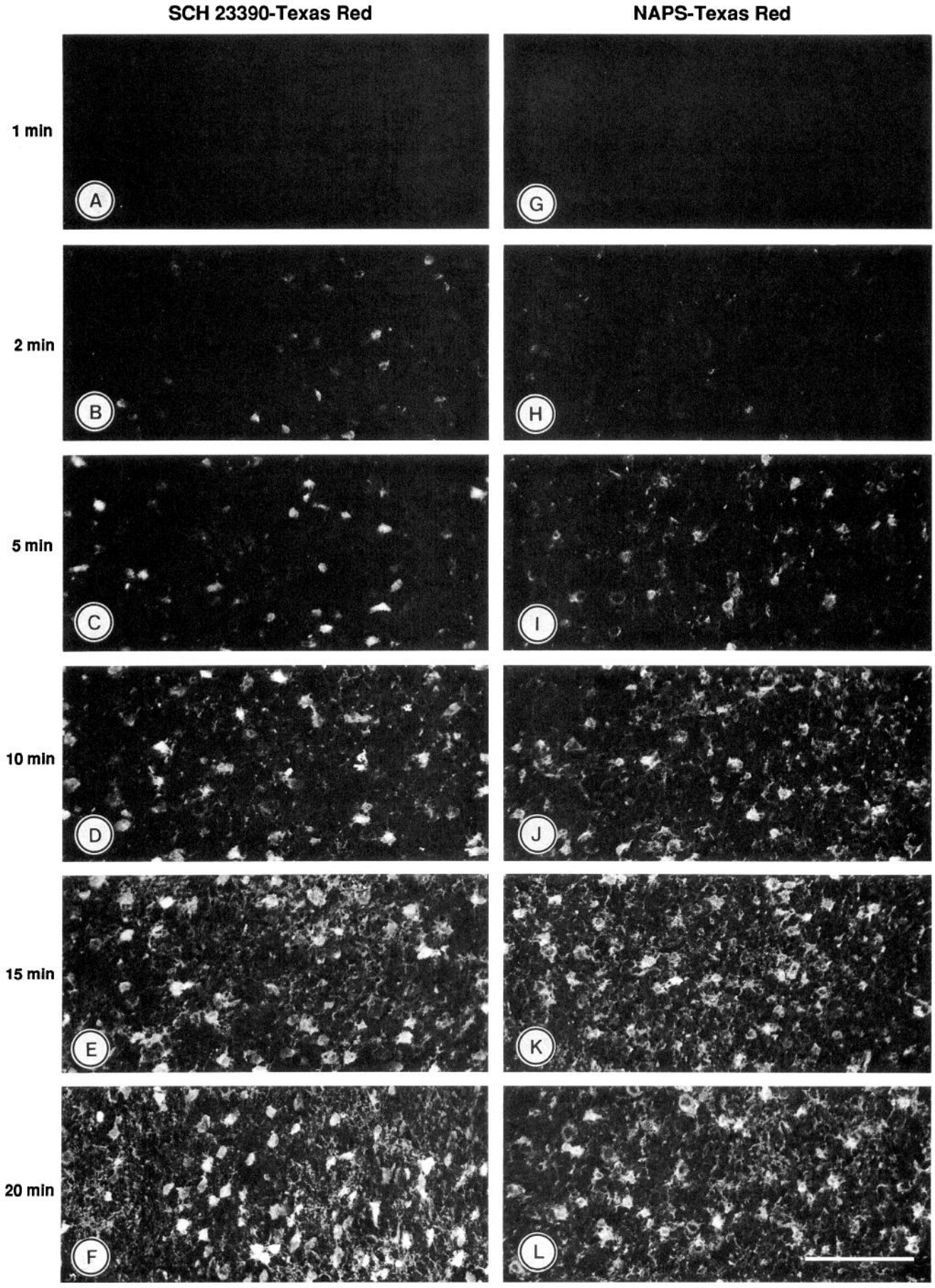
SCH 23390-Texas Red
NAPS-Texas Red
1 min
2 min
5 min
10 min
15 min
20 min
A
B
C
D
E
F
G
H
I
J
K
L

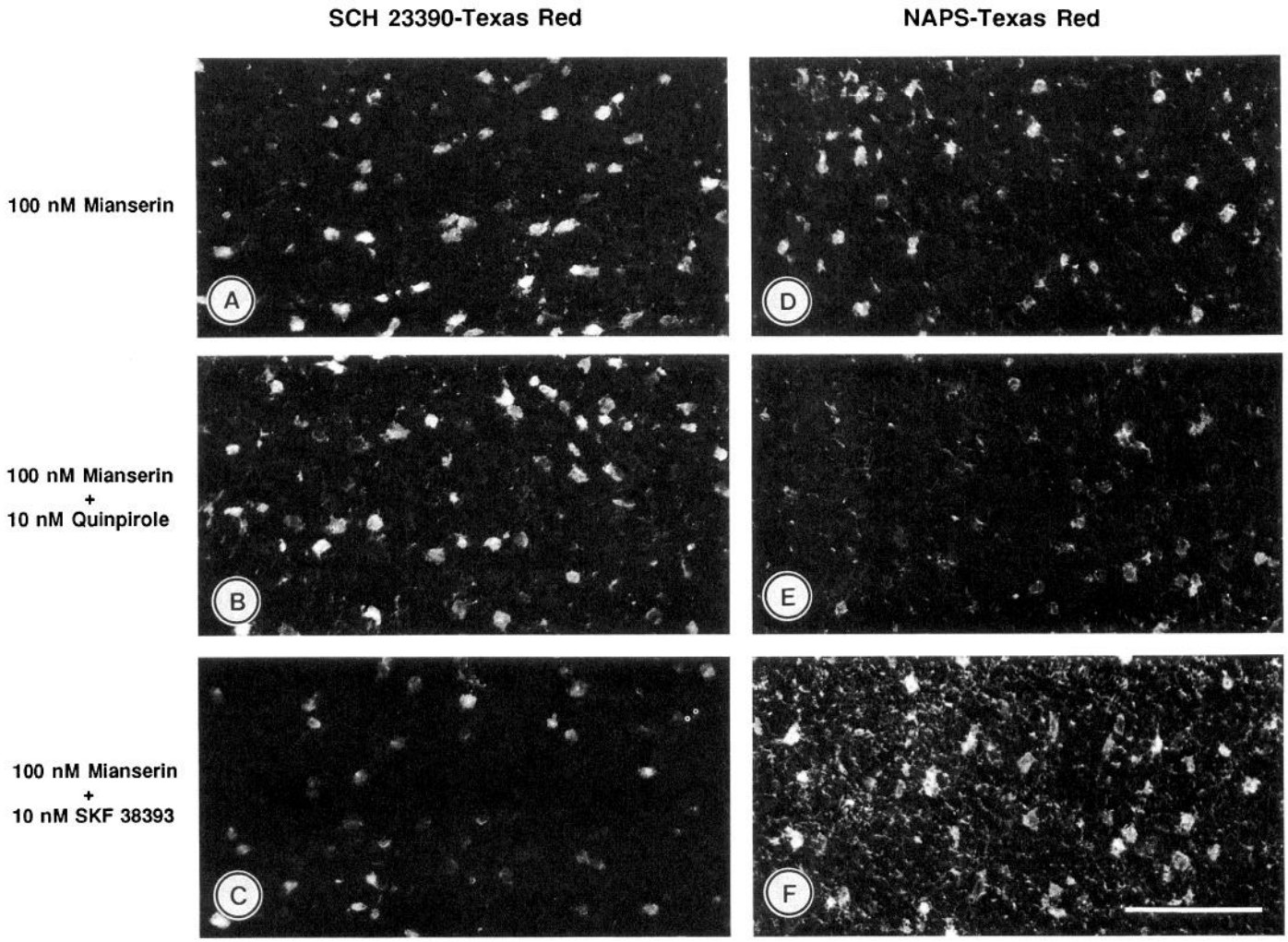

Figure 2. A series of photomicrographs from a competition and receptor specificity experiment showing the binding of SCH 23390–Texas red and NAPS–Texas red in the presence of either quinpirole or SKF 38393. *A*, SCH 23390–Texas red. *B*, SCH 23390–Texas red + 10 nM quinpirole. *C*, SCH 23390–Texas red + 10 nM SKF 38393. *D*, NAPS–Texas red. *E*, NAPS–Texas red + 10 nM quinpirole. *F*, NAPS–Texas red + 10 nM SKF 38393. Mianserin (100 nM) was present in all incubations. The binding of SCH 23390–Texas red is inhibited by SKF 38393, but not quinpirole, while binding of NAPS–Texas red is inhibited by quinpirole, but not SKF 38393. Scale bar, 100 μm.

fluorescent signal on cell bodies with minimal background fluorescence in neuropil.

Competition studies indicated that binding of fluorescently coupled ligands was selective for the dopamine D_1 and D_2 receptor subtypes. The effectiveness of the respective competitive inhibitors to inhibit binding of the fluorophore-coupled ligands was determined by visual analysis of the relative intensity of fluorescence emission illustrated in the photomicrograph series generated for each incubation in the presence of competitor. When 10 nM unlabeled SKF 38393 was added to the incubation, it substantially reduced the intensity of fluorescence when compared to sections incubated with SCH 23390–Texas red alone (Fig. 2). In sections incubated with NAPS–Texas red there was a similar reduction in the amount of fluorescence when 10 nM quinpirole was added to the medium (Fig. 2). SKF 38393 (10 nM) was ineffective in reducing the intensity of fluorescence seen with 100 nM NAPS–Texas red, while quinpirole (10 nM) did not inhibit the binding of SCH 23390–Texas red.

Distribution analysis

The relative frequency of cells showing both dopamine receptor–binding fluorescence and NSE-IR was compared in layer VI and subcortical white matter of mPFC (Fig. 3). This analysis demonstrated that fluorescence from both D_1 and D_2 dopamine receptor ligands was localized to neuronal cell bodies, while only a small proportion of neuroglial cells were labeled with fluoroprobe. In layer VI, the percentage of dopamine receptor–positive neurons that also showed corresponding NSE-IR was 91% for D_1-, and 78% for D_2-like receptor binding (Fig. 4). The density of D_1- and D_2-positive cells in layer VI was 22% and

←

Figure 1. A series of photomicrographs from an incubation time course experiment showing the binding of fluorescently coupled ligands for the dopamine D_1 and D_2 receptor binding sites in rat mPFC. *A–F*, 100 nM SCH 23390–Texas red; *G–L*, 100 nM NAPS–Texas red. *Numbers to the left* indicate the length of incubation expressed in minutes. Fluoroprobes for both the D_1 (*A–F*) and D_2 (*G–L*) receptor sites show a gradual increase of binding to cells between 1 and approximately 15 min of incubation. Scale bar, 100 μm.

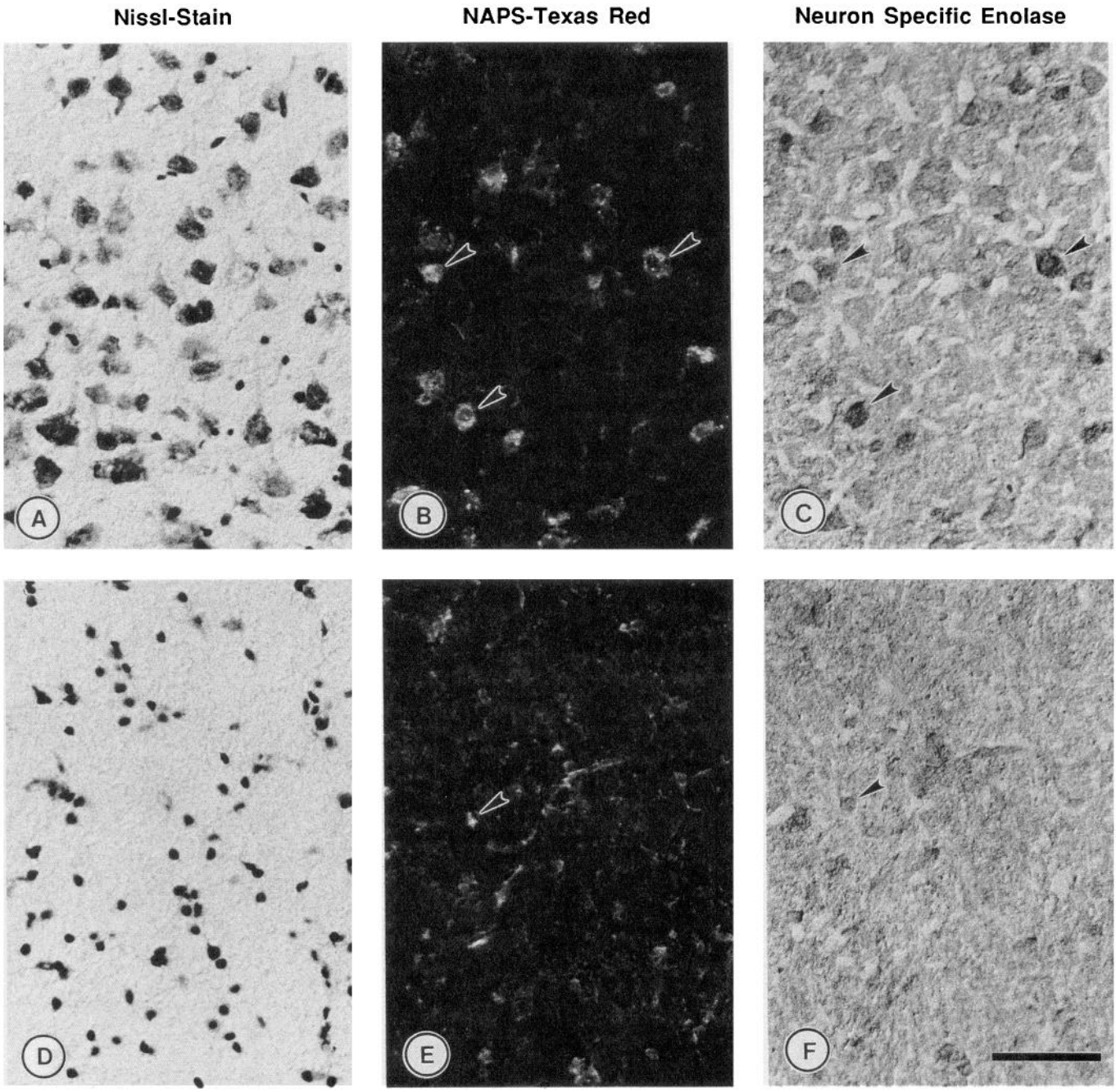

Figure 3. A series of photomicrographs showing the correlation between cells visualized with NAPS–Texas red and NSE-IR in layer VI of rat mPFC and in the underlying subcortical white matter. *A*, A representative adjacent Nissl-stained section showing the distribution of neuronal cell bodies in layer VI of rat mPFC. *B*, NAPS–Texas red binding to cells (*arrowheads*) in layer VI. *C*, A matched photographic field to *B* showing NSE-IR cell bodies (*arrowheads*) that correspond to receptor-positive cells. *D*, A representative adjacent Nissl-stained section showing abundant numbers of neuroglial cells in white matter below the cortical mantle of rat mPFC. *E*, NAPS–Texas red binding to some cells in white matter (*arrowhead*). *F*, A matched photographic field to *E* showing NSE-IR small cells (*arrowhead*) in white matter. In layer VI (*B, C*), *arrowheads* indicate examples of D_2 receptor–positive cells that also show NSE-IR in these matched photographic frames. In white matter (*E, F*), the *arrowhead* indicates an example of a small cell showing both NAPS–Texas red binding and NSE-IR in these matched photographic frames. Most receptor-positive cells in layer VI are probably neuronal cell bodies, while in white matter the few cells that show binding are predominantly glial in nature. Scale bar, 50 μm.

47%, respectively, of that for Nissl-stained neurons obtained in a similar region from an adjacent section. In the white matter beneath layer VI, the percentage of dopamine receptor–positive cells that also showed corresponding NSE-IR was 28% for D_1- and 49% for D_2-like receptor binding (Fig. 4).

An analysis of size distribution for cells showing D_1- and D_2-like receptor binding fluorescence was conducted in layer VI and the subcortical white matter, and the data were compared with the cell size distribution generated from adjacent Nissl-stained sections. The distribution of size for cells in layer VI showing D_1- or D_2-like receptor binding fluorescence was different for the respective receptor subtypes (Fig. 5). D_1 receptor–positive cells had a mean area (±SEM) of 77.8 ± 5.1 μm^2, with the majority (88%) of cells occurring in the size range of 41–

100 μm^2. This size range overlapped with that for nonpyramidal neurons measured from the Nissl-stained sections (Fig. 5). In contrast, cells showing D_2-like receptor binding fluorescence had a mean size of 108.2 ± 4.5 μm^2, with the majority (73%) of these cells occurring in the size range of 61–120 μm^2, which overlapped with both large nonpyramidal and small pyramidal neurons (Fig. 5). A large proportion (50%) of D_2 receptor–positive cells occurred in the size range of 100–200 μm^2 in which pyramidal neurons are exclusively found. The size range of most fluorescence-emitting cells in the subcortical white matter was 1–40 μm^2, overlapping with that for neuroglial cells; some of these cells may be small nonpyramidal neurons because 10% and 1% of D_1 and D_2 receptor–positive cells, respectively, had a size range of 41–60 μm^2. The latter range is similar to that for the smallest neurons seen in layer VI from the Nissl-stained sections.

The laminar distribution of neurons with D_1- or D_2-like receptor binding fluorescence was sampled from several receptor binding experiments (Figs. 6, 7). There were 147% and 88% more D_1 and D_2 receptor–positive cells, respectively, per 1000 μm^2 in layers V–VI versus layers II–III (Fig. 7). The contribution of 5-HT_2 receptor binding to the D_2-like binding fluorescence observed in superficial versus deep layers with NAPS–Texas red was evaluated and controlled for by adding a 5-HT_2 receptor blocking agent to the incubation solutions. In the presence of 100 nM mianserin, there was a decrease in the number of labeled cells per 1000 μm^2 in layers II–III (33%) and V–VI (17%) (Fig. 8). The overall pattern of more cells showing D_1-like and D_2-like receptor binding fluorescence in the deeper layers than in superficial ones was not altered by mianserin.

Discussion

Methodological considerations

The present study demonstrates the cellular localization and distribution of the dopamine D_1 and D_2 receptor subtypes in the mPFC of rat by using the high-affinity, fluorescently coupled ligands SCH 23390 and NAPS, respectively. A significant advantage of using such fluoroprobes for receptor binding in place of other methods, such as autoradiography, is its compatibility with other localization procedures such as immunocytochemistry. Toward this end, the use of these fluoroprobes enables rapid assessment of receptor localization (within 24 hr), a significant improvement over the extensive exposure times (2–8 weeks) required for using tritium-labeled ligands in conventional *in vitro* autoradiography. In order to establish the suitability of fluoroprobes for receptor binding in sections of intact tissue, however, it is necessary to determine that the binding characteristics of these modified ligands are consistent with accepted pharmacological parameters. In this regard, the initial focus of the present study was directed toward establishing appropriate binding conditions for receptor binding on glass-mounted tissue sections that could provide relatively reproducible and predictable results. The analysis of results from these experiments relied on the use of photomicrographs and necessitated that the photographic procedures, such as exposure times, development, and printing conditions, be carefully controlled and standardized.

An important consideration in applying fluorescently coupled ligands to localize cortical dopamine receptor binding sites was the method of tissue preparation. Initial attempts to localize the D_1- and D_2-like receptor binding fluorescence in rat mPFC employed tissue specimens that were minimally fixed with aldehyde, cryoprotected, and frozen. This method has proven to be compatible with standard procedures for the localization of many types of receptor binding sites (Young and Kuhar, 1979, 1980; Unnerstall et al., 1981; Vogt and Burns, 1988; Vogt et al., 1990) and also provides good preservation of morphological detail for light microscopic analysis (Benes et al., 1989). In the present study, tissues prepared in this manner showed marked variations in fluorescent emission intensity among different tissue

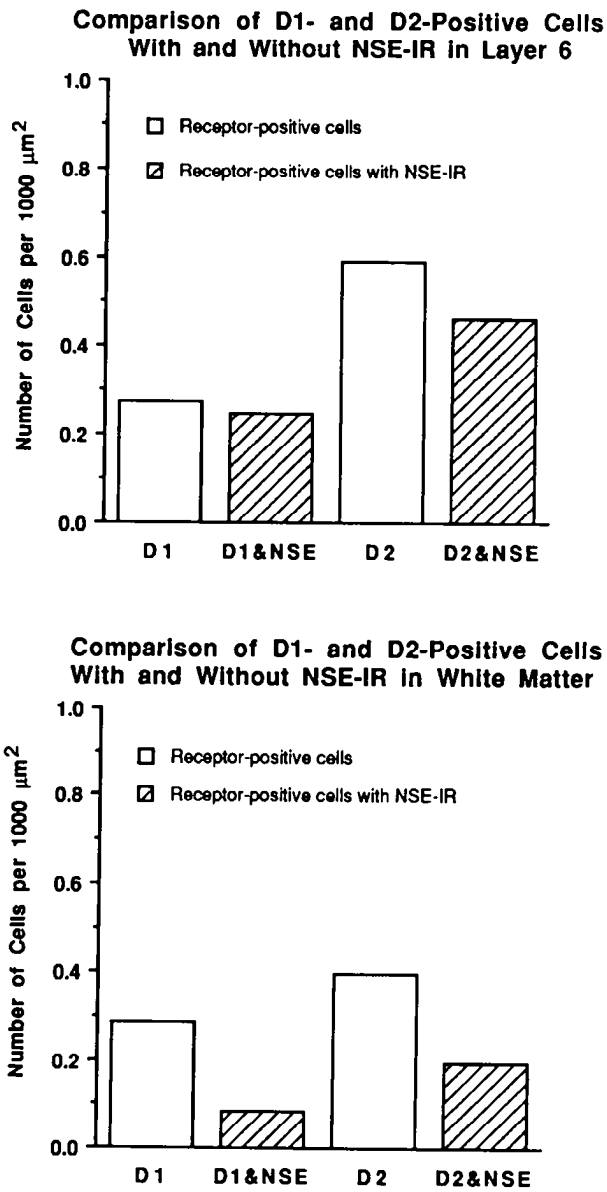

Figure 4. A comparison of cells showing binding of either fluorescently coupled D_1 or D_2 ligands and NSE-IR in layer VI or white matter of rat mPFC. Sections were first incubated with either SCH 23390–Texas red or NAPS–Texas red, and then photomicrographs taken, processed for the immunocytochemical localization of NSE, and again photographed. Cells first showing either D_1- or D_2-like binding (*open bars*) and later also NSE-IR (*hatched bars*) are shown for both layer VI and white matter. In layer VI, there is nearly complete overlap of both D_1- and D_2-positive cells with ones that are NSE-IR. In the white matter, most cells showing D_1-like ligand binding do not show NSE-IR, while about half of those showing D_2-like binding also show NSE-IR. These data suggest that the fluorescently coupled dopamine antagonist ligands bind predominantly to neuronal cell bodies in layer VI, while in white matter, cells similarly labeled are probably neuroglial cells.

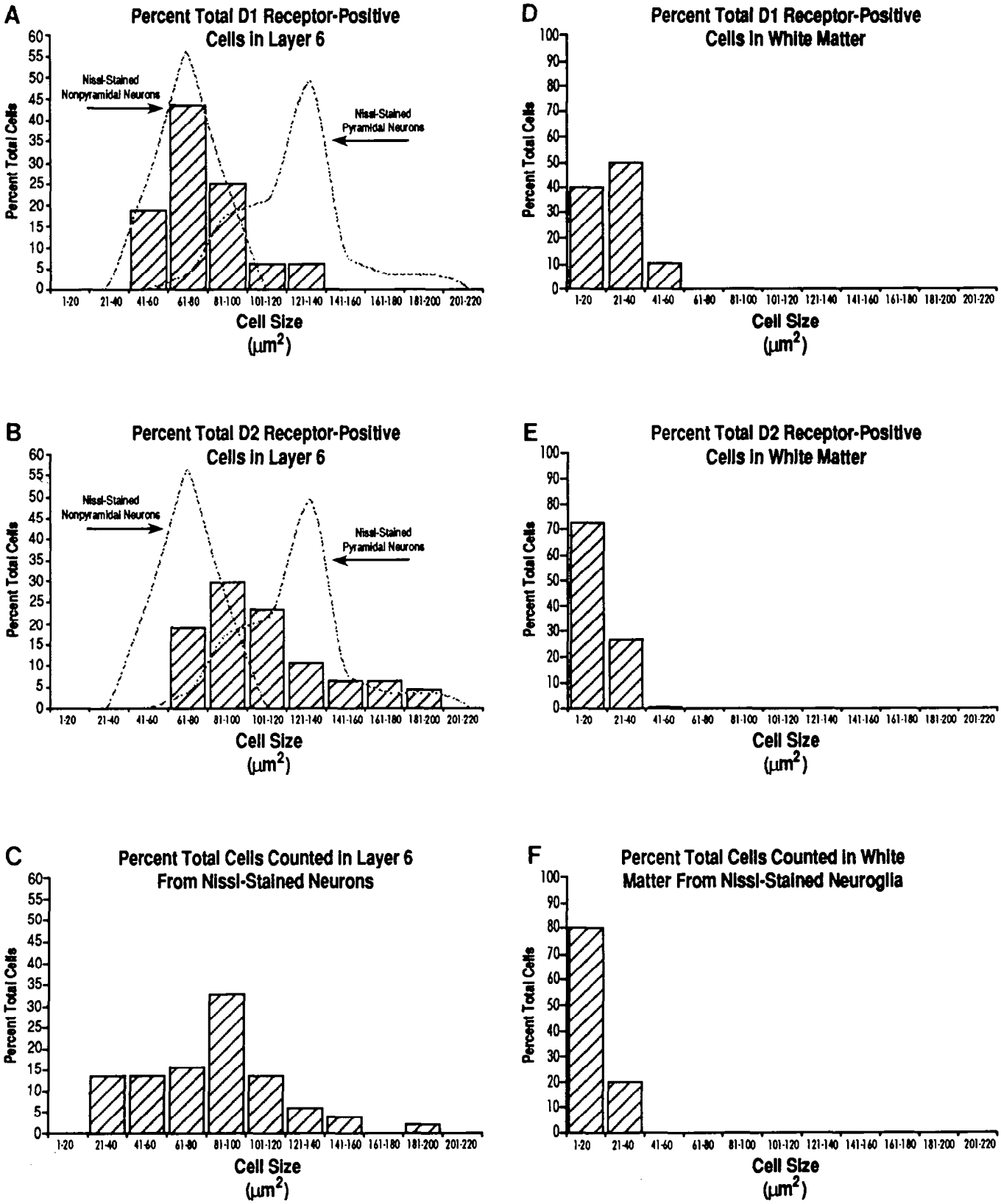

Figure 5. Histogram distributions for cell size in layer VI and white matter of mPFC. *A*, D_1-positive cells in layer VI. *B*, D_2-positive cells in layer VI. *C*, Nissl-stained neurons in layer VI. *D*, D_1-positive cells in white matter. *E*, D_2-positive cells in white matter. *F*, Nissl-stained neuroglial cells in white matter. In *A* and *B*, distribution curves for the size of pyramidal and nonpyramidal neurons have been superimposed on the histograms (*broken lines*). D_1-positive cells in layer VI have a range of sizes that overlaps with nonpyramidal neurons, while D_2-positive cells in layer VI have a broad distribution of sizes encompassing that for both large nonpyramidal and small pyramidal neurons. In white matter, D_1- and D_2-positive cells have a narrow size range that overlaps principally with neuroglial cells and, to a lesser extent, with some of the smallest nonpyramidal neurons.

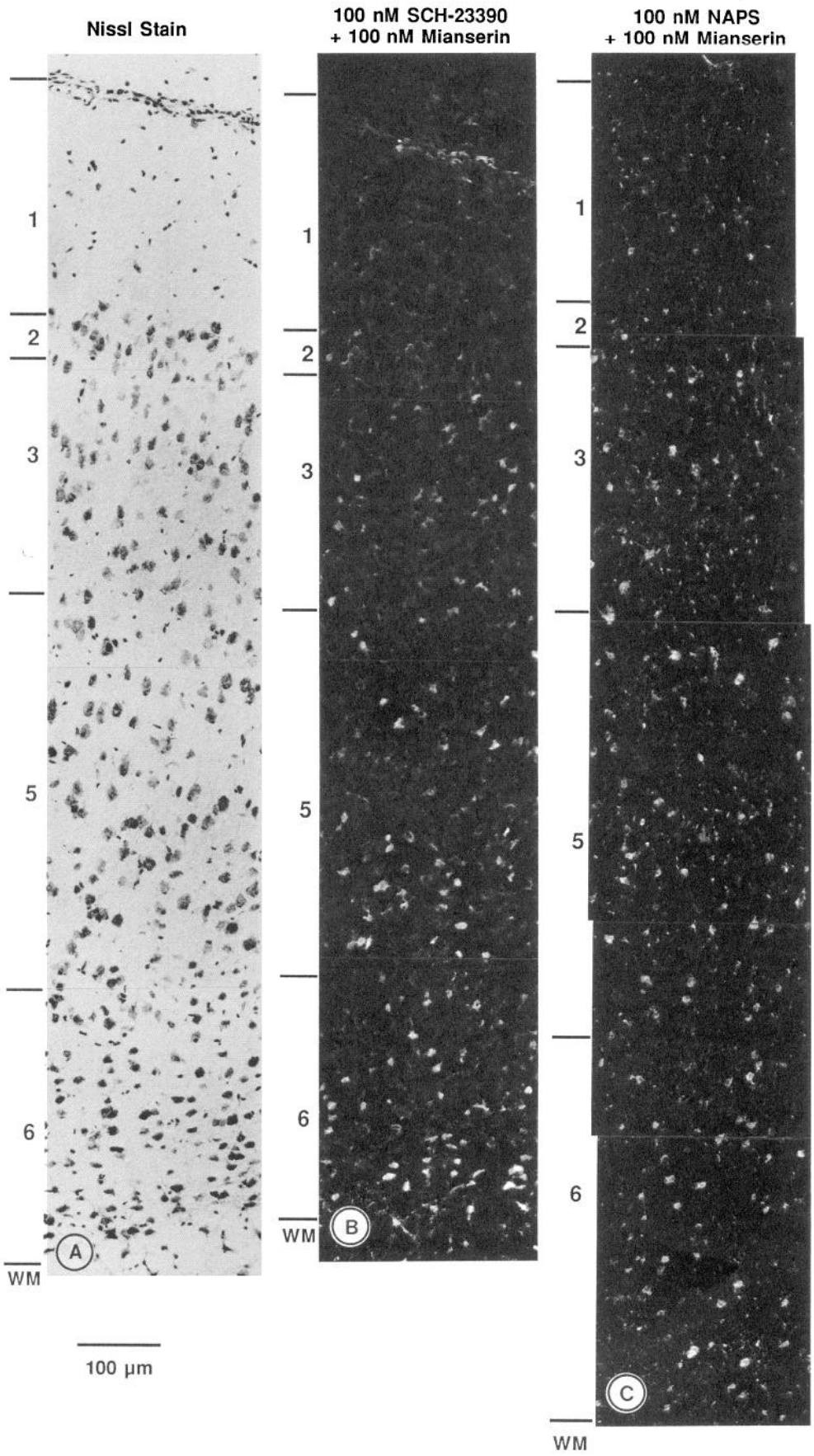

Figure 6. Photomontages of layers I–VI of rat mPFC. *A*, Representative Nissl-stained section showing the typical distribution of cells in mPFC. *B*, Fluorescent emissions from 100 nM SCH 23390–Texas red + 100 nM mianserin. *C*, Fluorescent emission from 100 nM NAPS–Texas red + 100 nM mianserin. Dopamine receptor–positive cell bodies are preferentially distributed in the deeper layers (cortical laminae identified to the left of each montage).

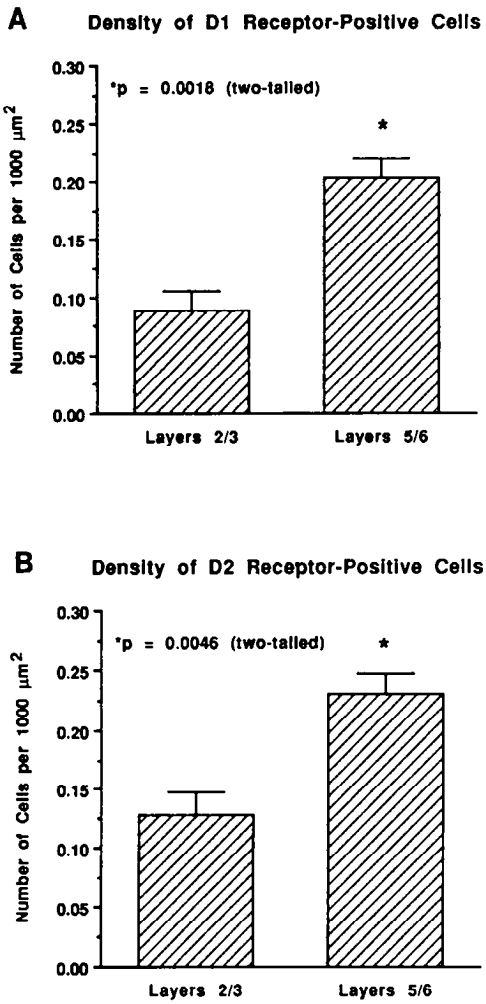

Figure 7. The density of D_1- (*A*) and D_2 (*B*) receptor–positive cells in superficial versus deep layers of rat mPFC (error bars = SEM). *A*, Cells binding SCH 23390–Texas red. *B*, Cells binding NAPS–Texas red. There are approximately twice as many D_1- and D_2 receptor–positive cell bodies in layers 5–6 than are present in layers II–III. Since there are more dopamine projections in layers V–VI than in II–III of mPFC, the distribution of receptor-positive cells parallels that for the termination of the cortical dopamine projection.

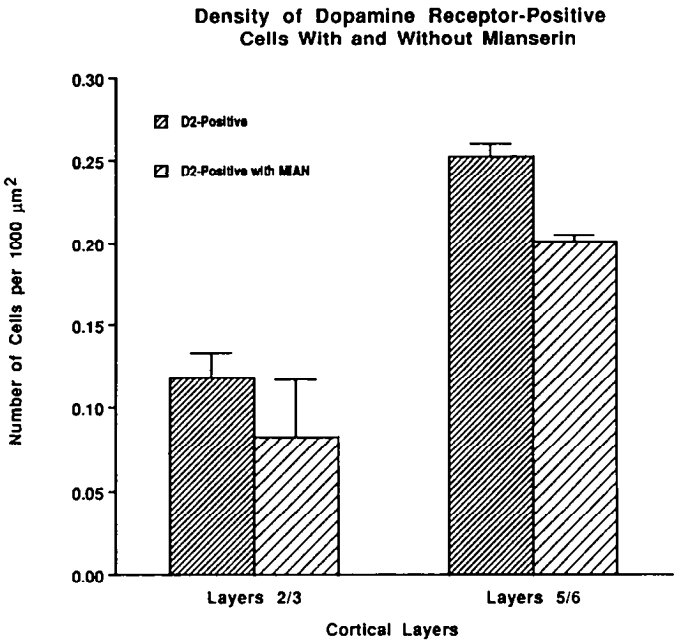

Figure 8. Histogram distributions showing the effect of 100 nM mianserin on the binding of NAPS–Texas red to cells in mPFC (error bars = SEM). Mianserin inhibits the nonspecific binding of NAPS–Texas red to cortical 5-HT_2 receptors. In the presence of mianserin there is a reduction in the number of cells identified as dopamine receptor positive. The largest effect is in the superficial layers, where the highest density of 5-HT_2 receptors is known to be localized.

sections treated in an identical fashion both within a single experiment and between different experiments. Subsequent studies demonstrated that these variations could be minimized by (1) eliminating the fixation and cryoprotection steps in tissue preparation and using fresh-frozen material, (2) briefly washing the tissues initially to remove endogenous ligand, (3) changing the buffer system from sodium phosphate to Tris-HCl, and (4) conducting all binding and washing procedures at 2°C. Another methodological concern in the present study was related to the long-term stability of these fluoroprobes. Unlike tritiated ligands that exhibit little change in their binding characteristics following extended storage intervals, the binding characteristics of the fluorescently coupled, dopamine-specific ligands were significantly affected by relatively brief storage times. When dissolved in DMSO and stored frozen at −20°C for up to 6 weeks, the fluoroprobes showed reproducible binding properties and emitted a bright signal. After 6 weeks of storage, there was increased variability in binding and the specific fluorescent signal on cell bodies decreased appreciably. It is also important to use pure grade, anhydrous DMSO for dissolving freshly obtained fluoroprobe in order to maintain appropriate ligand binding characteristics and fluorescent emission energy.

An important issue for the use of these fluoroprobes in sections of intact tissue was to optimize binding and support the selectivity of binding of the fluorescently coupled ligands to D_1 and D_2 dopamine receptors. Toward this end, several different studies were performed. There was a proportional rise in the apparent intensity of fluorescence emission as ligand concentration was varied from 10 to 100 nM: at 10 nM, fluorescence emission was undetectable even at 15 min incubation, while at a concentration of 100 nM, there were well-visualized cell bodies. This latter observation is consistent with previous reports in which a similar concentration was also found to be optimal for consistent and reproducible visualization of receptor binding localizations of similar fluorophore-coupled ligands (Ariano et al., 1989, 1991; Madras et al., 1990). Although a 100 nM concentration is considerably higher than the reported affinity values for these fluorescently coupled ligands, and may result in some loss of selectivity for the respective D_1 and D_2 receptor subtypes (Barton et al., 1991), this concentration was necessary to obtain fluorescent emission of sufficiently high energy to be consistently visualized and recorded on light-sensitive film.

In using the present fluoroprobes, it was also necessary to demonstrate linear binding characteristics as determined from kinetic studies. Following a 16 hr incubation with a 100 nM concentration of SCH 23390–Bodipy (Ariano et al., 1989), there was intense fluorescence throughout the entire section that obscured a potential signal from specific neuronal cell bodies. Kinetic experiments indicated that incubation for 1–15 min resulted in a linear increase of fluorescent signal on cell bodies. Beyond 15 min of incubation, fluorescent emission from the

neuropil increased gradually up to approximately 90 min, at which time the emission was no longer distinguishable from that on cell bodies. This characteristic of cell bodies to be visualized initially and then followed by an increase of fluorescence in the neuropil may be due to a combination of several factors. For example, it is possible that the dopamine receptor population on cell bodies may be of a higher density than that associated with neuronal processes in the neuropil. It is also possible that dopamine receptors on dendrites and spines, and possibly even autoreceptors (Roth, 1984) on dopamine terminals, may display different affinities for these fluoroprobes than those on cell bodies of the cortex. Since the goal of this study was to identify the types of cells that may express receptors for dopamine, it was important to visualize binding selectively on neuronal cell bodies. In this way, it will eventually be possible to combine the current localization procedure for receptors with one that can visualize markers for other intrinsic transmitter systems, so that the identity of these dopamine receptor–positive cells may be elucidated. It should be noted, however, that the data are equivocal regarding the presence of dopamine axosomatic synapses in cortex. Several electron microscopic studies provide evidence suggesting either the absence of such synaptic relations (Van Eden et al., 1987; Seguela et al., 1988) or their presence on pyramidal and possibly nonpyramidal cell soma (Goldman-Rakic et al., 1989; Verney et al., 1990). Interestingly, although these studies report a paucity of dopamine axosomatic synapses, they also note the frequent occurrence of dopamine axonal varicosities in close apposition to neuronal perikarya, suggesting the possibility that these terminals may exert a nonsynaptic action on neuronal cell bodies. We probably also have localized receptor molecules within the cytoplasmic compartment of cell bodies, but most, or even all of these may eventually be inserted in distal dendrites. This receptor pool would, nevertheless, have aided us in the identification of a preferential distribution of D_1 versus D_2 receptor subtypes with respect to nonpyramidal versus pyramidal cells. Nevertheless, we cannot exclude the possibility that some of the cell body labeling observed might reflect binding not to receptor molecules but, rather, to other nonreceptor proteins within the cytoplasm. With the technique employed here, it is not possible to exclude this latter possibility. Even so, such nonreceptor binding would have occurred in cells showing a laminar distribution similar to that for the mesocortical dopamine projection, suggesting that this potential pool might play a role in the mediation of dopamine effects on cortical neurons.

Although the parent ligands demonstrate relatively high affinity for dopamine receptors (Barton et al., 1991), it was necessary to evaluate the subtype selectivity of these fluorescently derivatized ligands in intact tissue sections. It has been reported that the coupling of a fluorophore moiety to these ligands can lower their affinity and receptor subtype selectivity (Barton et al., 1991). For this reason, the present study included a series of experiments in which the effects of the dopamine receptor agonists SKF 38393 and quinpirole were evaluated. These compounds produced little noticeable cross-inhibition for their respective opposite receptor subtype binding site. Low concentrations (10 nM) of the dopamine-selective agonists SKF 38393 and quinpirole were effective in reducing the binding of the fluorescently coupled, dopamine receptor–selective antagonists SCH 23390 and NAPS, respectively, but not vice versa. Although dopamine receptor–selective ligands coupled to the fluorophore Texas red have been reported to show a greater decrease in selectivity than with other fluorophores (Barton et al., 1991), the present results show that under the conditions employed here, receptor subtype specificity was adequately maintained when either the D_1 or D_2 ligands were derivatized with Texas red.

The dopamine receptor agonists SKF 38393 and quinpirole were selected for use in examining the subtype selectivity of the fluoroprobes based on the findings from initial experiments using either unlabeled agonists or antagonists, including SCH 23390 and spiperone. These studies indicated that the use of the agonists SKF 38393 and quinpirole produced the most reliable diminution of fluorescent signal through a series of several experiments. It is difficult to address specifically the reasons why these two agonists produced the most satisfactory result. There may be a variety of steric interactions between unlabeled antagonists and their counterparts conjugated to fluorescent moieties. The fact that there was an inhibitory effect by SKF 38393 and quinpirole with a concentration 10 times lower than that for the labeled ligand suggests that the fluorescently coupled ligands were selective for their respective receptor subtypes. Additional evidence in support of this conclusion is provided by several recent studies that have also demonstrated the specificity of similar fluoroprobes for D_1 and D_2 receptor binding sites in both intact tissue sections and striatal membrane suspensions (Ariano et al., 1989, 1991; Monsma et al., 1989; Barton et al., 1991).

Receptor localization and distribution considerations

Since the quantitative findings for the D_1 and D_2 dopamine receptor subtypes were very similar, the results obtained from these receptor binding studies will be considered together. There was a high degree of colocalization for fluorescence-emitting cell bodies with NSE-IR ones. This observation suggested strongly that some dopamine receptor binding sites may be present on neuronal cell bodies in mPFC. Some neurons in other dopaminoceptive regions also have been found to possess dopamine receptors. For example, it is thought that dopamine D_1 receptors may occur on postsynaptic neuronal cell bodies in adult rat striatum (Dubois et al., 1986) while D_2 receptors are located on neuronal somata in substantia nigra (Creese et al., 1983). Additional evidence from the present study supporting a localization of these receptors on cell bodies comes from the size analysis of fluoroprobe-positive cells in layer VI of mPFC. Notably, the size range of D_1 receptor–positive cells is similar to that of nonpyramidal neurons and the size range of D_2 receptor–positive cells overlaps with that for both large nonpyramidal and small pyramidal neurons. Interestingly, immunocytochemical studies of DARPP-32 (Ouimet et al., 1984; Berger et al., 1990), a dopamine- and cAMP-regulated phosphoprotein associated with dopaminoceptive neurons (Walaas and Greengard, 1984), indicate that the majority of neurons containing this protein in rat and monkey cortex display the morphological characteristics of pyramidal cells of varying sizes, although some have the characteristics of nonpyramidal neurons. In addition, in a recent report combining light and electron microscopic immunocytochemistry and Golgi impregnations, dopamine-containing axon terminals were found to form symmetric synapses on the soma, dendritic shafts, and spines of cortical pyramidal cells (Goldman-Rakic et al., 1989), although some terminals with immunoreaction product were also found on nonpyramidal cells with an appearance similar to basket neurons. These data taken to-

gether with the present findings suggest that dopamine D_1 and D_2 receptors may be differentially localized to a broad range of nonpyramidal versus large nonpyramidal and small pyramidal neuronal cell types, respectively. While some studies have suggested that DARPP-32–containing cells are primarily pyramidal neurons that express D_1 receptors, the present study indicates that in cortex the D_1 subtype may be preferentially localized to nonpyramidal elements. The colocalization of DARPP-32 with D_1 receptors has been inferred from regional distribution analyses in subcortical areas (Walaas and Greengard, 1984). Based on the present findings, the proposed association of D_1 receptors with DARPP-32–containing pyramidal cells may not be the case in cortex where the dopamine system also shows unique functional properties not observed in subcortical regions. For example, there is a selective response of mesoprefrontal dopamine afferents (originating from A10 cell bodies) to footshock stress (Thierry et al., 1976; Lavielle et al., 1978; Tam and Roth, 1985; Roth et al., 1988; Deutch and Roth, 1990). An electrophysiological study has shown that both D_1 and D_2 agonists can induce inhibitory responses and inhibitory responses followed by excitatory responses in dopamine-sensitive neurons of rat mPFC (Sesack and Bunney, 1989). These findings are compatible with a model in which D_1 and D_2 receptors localized on interneurons and pyramidal cells, respectively, give rise to opposing influences on neuronal firing, possibly through combined disinhibitory and inhibitory mechanisms. It should be pointed out, however, that inhibitory responses were only recorded in 7% of the pyramidal cells studies; however, the D_2 selective antagonist sulpiride specifically attenuated this dopamine-induced inhibition of pyramidal neurons (Sesack and Bunney, 1989). Thus, the selective effects of dopaminergic afferents on mPFC may be mediated through a complex set of interactions among intrinsic cortical elements.

Several recent reports provide evidence to support the idea of colocalization of dopamine receptor subtypes on some of the same cells and, specifically, suggest a synergistic interaction between the D_1 and D_2 receptors in striatal medium spiny neurons (Walters et al., 1987; Bertorello et al., 1990; Strange, 1991). Although the present results suggest that there may be a differential distribution of D_1- and D_2-like receptor binding fluorescence on different populations of cortical neurons, there nevertheless was some overlap for the two receptor subtypes on nonpyramidal neurons in the size range of 80–100 μm^2. In order to ascertain specifically whether D_1 and D_2 receptors are coexpressed on a subpopulation of cortical dopaminoceptive neurons, it will be desirable to use fluorescently coupled ligands at lower concentrations that will ensure greater selectivity for the respective receptor subtypes. Toward this end, quantitative fluorescence densitometry will be needed for the respective probes because binding at lower concentrations of ligand will be below the limits of sensitivity of conventional photomicrographic techniques. In addition, it is also of interest to note that the labeling characteristics of the respective fluoroprobes, as demonstrated in Figures 1–3, suggest the possibility of probe localization both intracellularly and on the cell surface. At the present level of magnification and image resolution, however, it is not possible to determine accurately the exact nature of such differences in visualization of the fluoroprobes. In order to explore this question further, it will be necessary to combine the use of low concentrations of fluoroprobe with the use of confocal microscopy that can provide the image resolution necessary to determine better the subcellular localization of these probes.

Analysis of the laminar distribution of D_1- and D_2-like receptor binding fluorescence in the present study showed cells with fluorescent emission present in layers II–VI. There was a significantly higher density of these cells preferentially distributed in layers V and VI than in the superficial laminae. This laminar gradient in the density of neurons showing D_1- and D_2-like receptor binding fluorescence in mPFC is consistent with the known distribution of the mesocortical projection (Emson and Koob, 1978; Lindvall and Bjorklund, 1978; Thierry et al., 1978), dopamine-containing fibers (Van Eden et al., 1987), DARPP-32–immunoreactive cells (Ouimet et., 1984; Berger et al., 1990), and DARPP-32 mRNA (Schalling et al., 1990). Furthermore, the distribution of cells showing fluorescence reported in this study is also consistent with the evidence provided from numerous autoradiographic studies in rat that show a corresponding laminar density gradient of D_1 and D_2 receptors in the anteromedial cortex, where the highest receptor density is preferentially localized in the deeper layers (Klemm et al., 1979; Dawson et al., 1985, 1986; Dubois et al., 1986; Savasta et al., 1986; Charuchinda et al., 1987; Richfield et al., 1989). It should also be noted that coincubation of NAPS–Texas red with 100 nM mianserin decreased the numbers of labeled cells through the depth of the cortex, but this effect was greatest in the superficial layers (see Fig. 5). The distribution pattern of D_2 receptor–positive cells shown here does not correspond to the known distribution of serotonergic afferents (Lidov et al., 1980) or 5-HT_2 receptors (Pazos et al., 1985) since, in the anterior cingulate cortex, the highest density of each is in the superficial layers and lowest density is in layer VI. Thus, taking into account their specific binding characteristics and their ability to label cells with a distribution similar to that of the mesocortical dopamine system, the fluorescently coupled, high-affinity dopamine antagonists used in this study appear to be useful probes for the investigation of the cellular distribution of D_1 and D_2 receptors in sections of intact tissue.

It is noteworthy that there was a small percentage of cells beneath the cortical mantle that also was found to have D_1- and D_2-like receptor binding fluorescence. As determined from the cell size distribution studies, the great majority of these receptor-positive cells fell into the size category of less than 40 μm^2, which corresponds to the size range of glial cells measured in Nissl-stained sections. A few such cells also showed some D_1-like receptor binding fluorescence and D_2-like receptor binding fluorescence in layer VI as well. A possible explanation for this finding comes from biochemical, electrophysiological, and autoradiographic receptor binding studies (Hosli and Hosli, 1986, 1988) suggesting that some astrocytes may possess receptors for dopamine and other biogenic amines. To date, there is little information regarding the functional role of such proposed glial receptors, although it has been suggested that such receptors might be involved in the regulation of second messengers such as cAMP (Hosli and Hosli, 1988).

Recent investigations have demonstrated that there may also be other, generally less prevalent, dopamine receptor subtypes, including D_2-like D_3 (Sokoloff et al., 1990) and D_4 (Van Tol et al., 1991) forms as well as a D_1-like D_5 (Sunahara et al., 1991) form. The heterogeneous forms of dopamine receptor subtypes could theoretically be associated with different cell types, including non-neuronal ones. Accordingly, the possibility must be considered that the D_1- and D_2-like receptor binding fluorescence noted on presumptive glial cells within and below layer VI could be attributable to the D_3, D_4, or D_5 subtypes; however,

specific probes for these receptors will be needed to resolve this question.

In conclusion, using a high-resolution, fluoroprobe receptor binding technique under carefully controlled conditions, the present study has demonstrated a localization of dopamine D_1 and D_2 receptor subtypes to neurons in the cortical mantle of rat mPFC. The fact that the deep cortical layers had the highest density of receptor-positive cells is consistent with the known distribution of various markers for the mesocortical projection and suggests that fluorophore-labeled ligands have visualized functionally relevant D_1 and D_2 receptor binding activity. The different size distributions observed for cells showing D_1- or D_2-like receptor–binding fluorescence indicate that different neuronal types probably express specific subtypes of dopamine receptor binding proteins, although overlap within some neurons may well occur. The present findings may contribute to the further understanding of how the dopamine system is integrated with intrinsic cortical neurons and their respective neurotransmitter systems.

References

Altar CA, O'Neil S, Walter RJ, Marshall JF (1985a) Brain dopamine and serotonin receptor sites revealed by digital subtraction autoradiography. Science 228:597–600.

Altar CA, Kim H, Marshall JF (1985b) Computer imaging and analysis of dopamine (D_2) and serotonin (S_2) binding sites in rat basal ganglia or neocortex labeled by [^{3}H]spiroperidol. J Pharmacol Exp Ther 233: 527–538.

Ariano MA, Monsma FJ, Barton AC, Kang HC, Haugland RP, Sibley DR (1989) Direct visualization and cellular localization of D1 and D2 dopamine receptors in rat forebrain by use of fluorescent ligands. Proc Natl Acad Sci USA 86:8570–8574.

Ariano MA, Kang HC, Haugland RP, Sibley DR (1991) Multiple fluorescent ligands for dopamine receptors. II. Visualization in neural tissues. Brain Res 547:208–222.

Bacopoulos NG, Spokes EG, Bird ED, Roth RH (1979) Antipsychotic drug action in schizophrenia patients: effects of cortical dopamine metabolism after long-term treatment. Science 205:405–407.

Barton AC, Kang HC, Rinaudo MS, Monsma FJ, Stewart-Fram RM, Macinko JA, Haugland RP, Ariano MA, Sibley DR (1991) Multiple fluorescent ligands for dopamine receptors. I. Pharmacological characterization and receptor selectivity. Brain Res 547:199–207.

Benes FM, Vincent SL, SanGiovanni JP (1989) High resolution imaging of receptor binding in analyzing neuropsychiatric diseases. Biotechniques 7:970–979.

Berger B (1977) Histochemical identification and localization of dopaminergic axons in rat and human cerebral cortex. In: Advances in biochemical psychopharmacology, Vol 16 (Costa E, Gessa GL, eds), pp 13–20. New York: Raven.

Berger B, Febvret A, Greengard P, Goldman-Rakic PS (1990) DARPP-32, a phosphoprotein enriched in dopaminoceptive neurons bearing dopamine D1 receptors: distribution in the cerebral cortex of the newborn and adult rhesus monkey. J Comp Neurol 299:327–348.

Berman KF, Zec RF, Weinberger DR (1986) Physiologic dysfunction of dorsolateral prefrontal cortex in schizophrenia. II. Role of neuroleptic treatment, attention, and mental effort. Arch Gen Psychiatry 43:126–135.

Bertorello AM, Hopfield JF, Aperia A, Greengard P (1990) Inhibition by dopamine of ($Na^+ + K^+$)ATPase activity in neostriatal neurons through D_1 and D_2 dopamine receptor synergism. Nature 347:386–388.

Boyson SJ, McGonigle P, Molinoff PB (1986) Quantitative autoradiographic localization of the D_1 and D_2 subtypes of dopamine receptors in rat brain. J Neurosci 6:3177–3188.

Camps M, Cortes R, Gueye B, Probst A, Palacios JM (1989) Dopamine receptors in human brain: autoradiographic distribution of D_2 sites. Neuroscience 28:275–290.

Camus A, Javoy-Agid F, Dubois A, Scatton B (1986) Autoradiographic localization and quantification of dopamine D_2 receptors in normal human brain with [^{3}H]*N*-*n*-propylnorapomorphine. Brain Res 375: 135–149.

Carlsson A (1978a) Does dopamine have a role in schizophrenia? Biol Psychiatry 13:3–21.

Carlsson A (1978b) Antipsychotic drugs, neurotransmitters, and schizophrenia. Am J Psychiatry 135:164–173.

Charuchinda C, Supavilai P, Karobath M, Palacios JM (1987) Dopamine D_2 receptors in the rat brain: autoradiographic visualization using a high-affinity selective agonist ligand. J Neurosci 7:1352–1360.

Cortes R, Gueye B, Pazos A, Probst A, Palacios JM (1989) Dopamine receptors in human brain: autoradiographic distribution of D_1 sites. Neuroscience 28:263–273.

Creese I, Sibley DR, Hamblin MW, Leff SE (1983) The classification of dopamine receptors: relation to radioligand binding. Annu Rev Neurosci 6:43–71.

Dawson TM, Gehlert DR, Yamamura HI, Barnett A, Wamsley JK (1985) D-1 dopamine receptors in the rat brain: autoradiographic localization using [^{3}H]SCH 23390. Eur J Pharmacol 108:323–325.

Dawson TM, Barone P, Sidhu A, Wamsley JK, Chase TN (1986) Quantitative autoradiographic localization of D-1 dopamine receptors in the rat brain: use of the iodinated ligand [^{125}I]SCH 23982. Neurosci Lett 68:261–266.

Dawson TM, McCabe RT, Stensaas SS, Wamsley JK (1987) Autoradiographic evidence of [^{3}H]SCH 23390 binding sites in human prefrontal cortex (Brodmann's area 9). J Neurochem 49:789–796.

De Keyser J, Claeys A, De Backer J-P, Ebinger G, Roels F, Vauquelin G (1988) Autoradiographic localization of D_1 and D_2 dopamine receptors in the human brain. Neurosci Lett 91:142–147.

Deutch AY, Roth RH (1990) The determinants of stress-induced activation of the prefrontal cortical dopamine system. Prog Brain Res 85:367–403.

Dubois A, Savasta M, Curet O, Scatton B (1986) Autoradiographic distribution of the D_1 agonist [^{3}H]SKF 38393, in the rat brain and spinal cord. Comparison with the distribution of D_2 dopamine receptors. Neuroscience 19:125–137.

Emson PC, Koob GF (1978) The origin and distribution of dopamine-containing afferents to the rat frontal cortex. Brain Res 142:249–267.

Giros B, Sokoff B, Martres M-P, Schwartz J-C (1990) Two D_2 dopamine receptor isoforms generated via alternative mRNA splicing: regional distribution and effects of haloperidol treatment. Eur J Pharmacol 183:1619.

Goldman-Rakic PS, Leranth C, Williams SM, Mons N, Geffard M (1989) Dopamine synaptic complex with pyramidal neurons in primate cerebral cortex. Proc Natl Acad Sci USA 86:9015–9019.

Herkenham M (1988) Receptor autoradiography: optimizing anatomical resolution. In: Receptor localization ligand autoradiography (Leslie FM, Altar CA, eds), pp 37–38. New York: Liss.

Hess EJ, Creese I (1987) Biochemical characterization of dopamine receptors. In: Dopamine receptors, pp 1–27. New York: Liss.

Hosli E, Hosli L (1986) Binding sites for [^{3}H]dopamine and dopamine-antagonists on cultured astrocytes of rat striatum and spinal cord: an autoradiographic study. Neurosci Lett 65:177–182.

Hosli L, Hosli E (1988) Electrophysiologic and autoradiographic evidence for receptors for biogenic amines on astrocytes in explant cultures of rat CNS. In: Glial cell receptors (Kimelberg HK, ed), pp 77–93. New York: Raven.

Kebabian JW, Calne DB (1979) Multiple receptors for dopamine. Nature 277:93–96.

Kety SS, Matthysse S (1972) Prospects for research on schizophrenia. An overview. Neurosci Res Bull 10:456–467.

Klemm N, Murrin LC, Kuhar MJ (1979) Neuroleptic and dopamine receptors: Autoradiographic localization of [^{3}H]spiperone in rat brain. Brain Res 169:1–9.

Kohler C, Radesater A-C (1986) Autoradiographic visualization of dopamine D-2 receptors in the monkey brain using the selective benzamide [^{3}H]raclopride. Neurosci Lett 66:85–90.

Lavielle S, Tassin J-P, Thierry A-M, Blanc G, Herve D, Barthelemy C, Glowinski J (1978) Blockade by benzodiazepines of the selective high increase in dopamine turnover by stress in mesocortical dopaminergic neurons of the rat. Brain Res 168:585–594.

Lewis DA, Foote SL, Goldstein M, Morrison JH (1988) The dopaminergic innervation of monkey prefrontal cortex: a tyrosine hydroxylase immunohistochemical study. Brain Res 449:225–243.

Lidov HGW, Grzanna R, Molliver ME (1980) The serotonin innervation of the cerebral cortex in the rat—an immunocytochemical analysis. Neuroscience 5:207–227.

Lidow MS, Goldman-Rakic PS, Rakic P, Innis RB (1989) Dopamine

D_2 receptors in the cerebral cortex: distribution and pharmacological characterization with [^{3}H]raclopride. Proc Natl Acad Sci USA 86: 6412–6416.

Lindvall O, Bjorklund A (1978) Anatomy of the dopaminergic neuron systems in the rat brain. In: Advances in biochemical psychopharmacology, Vol 19 (Roberts PJ, Woodruff GN, Iversen LL, eds), pp 1–23. New York: Raven.

Liskowsky DR, Potter LT (1985) D-2 dopamine receptors in the frontal cortex of rat and human. Life Sci 36:1551–1559.

Madras BK, Canfield DR, Pfaelzer C, Vittimberga FJ, DiFiglia M, Aronin N, Bakthavachalam V, Baindur N, Neumeyer JL (1990) Fluorescent and biotin probes for dopamine receptors: D_1 and D_2 receptor affinity and selectivity. Mol Pharmacol 37:833–839.

Matsumoto T, Uchimura H, Hirano M, Kem JS, Yokoo H, Shimomuro M, Nakahara T, Inoue K, Oomagari K (1983) Differential effects of acute and chronic administration of haloperidol on homovanillic acid levels in discrete dopaminergic areas of the brain. Eur J Pharmacol 89:27–33.

Meltzer HY, Stahl SM (1976) The dopamine hypothesis of schizophrenia: a review. Schizophr Bull 2:19–76.

Monsma FJ, Barton AC, Kang HC, Brassard DL, Haugland RP, Sibley DR (1989) Characterization of novel florescent ligands with high affinity for D_1 and D_2 dopaminergic receptors. J Neurochem 52:1641–1644.

Ouimet CC, Miller PE, Hemmings HC, Walaas SI, Greengard P (1984) DARP-32, a dopamine- and adenosine 3′:5′-monophosphate-regulated phosphoprotein enriched in dopamine-innervated brain regions. III. Immunocytochemical localization. J Neurosci 4:111–124.

Palacios JM, Niehoff DL, Kuhar MJ (1981) [^{3}H]spiperone binding sites in brain: autoradiographic localization of multiple receptors. Brain Res 213:277–289.

Paxinos G, Watson C (1986) The rat brain in stereotaxic coordinates. New York: Academic.

Pazos A, Cortes R, Palacios JM (1985) Quantitative autoradiographic mapping of serotonin receptors in the rat brain. II. Serotonin-2 receptors. Brain Res 346:231–249.

Richfield EK, Young AB, Penney JB (1987) Comparative distribution of dopamine D-1 and D-2 receptors in the basal ganglia of turtles, pigeons, rats, cats, and monkeys. J Comp Neurol 262:446–463.

Richfield EK, Penny JB, Young AB (1989) Anatomical and affinity state comparisons between dopamine D_1 and D_2 receptors in the rat central nervous system. Neuroscience 30:767–777.

Roth RH (1984) CNS dopamine autoreceptors: distribution, pharmacology, and function. Ann NY Acad Sci 430:27–53.

Roth RH, Tam S-Y, Ida Y, Yang J-X, Deutch AY (1988) Stress and the mesocorticolimbic dopamine systems. Ann NY Acad Sci 537: 138–147.

Savasta M, Dubois A, Scatton B (1986) Autoradiographic localization of D_1 dopamine receptors in the rat brain with [^{3}H]SCH 23390. Brain Res 375:291–301.

Schalling M, Djurfeldt M, Hokfelt T, Ehrlich M, Kurihara T, Greengard P (1990) Distribution and cellular localization of DARPP-32 mRNA in rat brain. Mol Brain Res 7:139–149.

Seeman P (1981) Brain dopamine receptors. Pharmacol Rev 32:229–313.

Seguela P, Watkins KC, Descarries L (1988) Ultrastructural features of dopamine axon terminals in the anteromedial and the suprarhinal cortex of adult rat. Brain Res 442:11–22.

Sesack SR, Bunney BS (1989) Pharmacological characterization of the receptor mediating electrophysiological responses to dopamine in the rat medial prefrontal cortex: a microiontophoretic study. J Pharmacol Exp Ther 248:1323–1333.

Sokoloff P, Giros B, Martres M-P, Bouthenet M-L, Schwartz J-C (1990) Molecular cloning and characterization of a novel dopamine receptor (D_3) as a target for neuroleptics. Nature 347:146–151.

Stoof JC, Kebabian JW (1984) Two dopamine receptors biochemistry, physiology and pharmacology. Life Sci 35:2281–2296.

Strange PG (1991) D1/D2 dopamine receptor interaction at the biochemical level. Trends Pharmacol Sci 12:48–49.

Sunahara RK, Guan H-C, O'Dowd BF, Seeman P, Lauier LG, Ng G, George SR, Torchia J, Van Tol HHM, Niznik HB (1991) Cloning of the gene for a human dopamine D_5 receptor with higher affinity for dopamine than D_1. Nature 350:614–619.

Tam S-Y, Roth RH (1985) Selective increase in dopamine metabolism in the prefrontal cortex by the anxiogenic beta-carboline FG 7142. Biochem Pharmacol 34:1595–1598.

Thierry AM, Tassin J-P, Blanc G, Glowinski J (1976) Selective activation of the mesocortical dopamine system by stress. Nature 263: 242–243.

Thierry AM, Tassin J-P, Blanc G, Glowinski J (1978) Studies on mesocortical dopamine systems. In: Advances in biochemical psychopharmacology, Vol 19 (Roberts PJ, Woodruff GN, Iversen LL, eds), pp 205–216. New York: Raven.

Unnerstall JR, Kuhar MJ, Niehoff DL, Palacios MM (1981) Gamma-aminobutyric acid (GABA) receptors: evidence from a quantitative autoradiographic study. J Pharmacol Exp Ther 218:797–804.

Van Eden CG, Hoorneman EMD, Buijs RM, Matthijssen MAH, Gefard M, Uylings HBM (1987) Immunocytochemical localization of dopamine in the prefrontal cortex of the rat at the light and electron microscopic level. Neuroscience 22:849–862.

Van Tol HHM, Bunzow JR, Guan H-C, Sunahara RK, Seeman P, Niznik HB, Civelli O (1991) Cloning of the gene for a human dopamine D_4 receptor with high affinity for the antipsychotic clozapine. Nature 350:610–614.

Verney C, Alvarez C, Geffard M, Berger B (1990) Ultrastructural double-labelling study of dopamine terminals and GABA-containing neurons in rat anteromedial cerebral cortex. Eur J Neurosci 2:960–972.

Vogt BA, Burns DL (1988) Experimental localization of muscarinic receptor subtypes to cingulate cortical afferents and neurons. J Neurosci 8:643–652.

Vogt BA, Plager MD, Crino PB, Bird ED (1990) Laminar distributions of muscarinic acetylcholine, serotonin, GABA and opioid receptors in human posterior cingulate cortex. Neuroscience 36:165–174.

Walaas SI, Greengard P (1984) DARPP-32, a dopamine- and adenosine 3′:5′-monophosphate-regulated phosphoprotein enriched in dopamine-innervated brain regions. I. Regional and cellular distribution in the rat brain. J Neurosci 4:84–98.

Walters JR, Bergstrom DA, Carlson JH, Chase TN, Braun AR (1987) D_1 dopamine receptor activation is required for postsynaptic expression of D_2 agonist effects. Science 236:719–722.

Young WS, Kuhar MJ (1979) A new method for receptor autoradiography: [^{3}H]opioid receptors in rat brain. Brain Res 179:225–270.

Young WS, Kuhar MJ (1980) Radiohistochemical localization of benzodiazepine receptors in rat brain. J Pharmacol Exp Ther 212:337–346.

Zhou Q-Y, Grandy DK, Kushner JA, Van Tol HHM, Cone R, Pribnow D, Salon J, Bunzow JR, Civelli O (1990) Cloning and expression of human and rat D_1 dopamine receptor. Nature 347:76–79.